



HAL
open science

A sustainable fungal microbial fuel cell (FMFC) for the bioremediation of acetaminophen (APAP) and its main by-product (PAP) and energy production from biomass

M. Pontié, E. Jaspard, C. Friant, J. Kilani, A. Fix-Tailler, Christophe Innocent, D. Chery, S.F. Mbokou, A. Somrani, Benoît Cagnon, et al.

► To cite this version:

M. Pontié, E. Jaspard, C. Friant, J. Kilani, A. Fix-Tailler, et al.. A sustainable fungal microbial fuel cell (FMFC) for the bioremediation of acetaminophen (APAP) and its main by-product (PAP) and energy production from biomass. *Biocatalysis and Agricultural Biotechnology*, 2019, 22, pp.101376. 10.1016/j.bcab.2019.101376 . hal-02322600

HAL Id: hal-02322600

<https://hal.science/hal-02322600>

Submitted on 20 Jul 2022

HAL is a multi-disciplinary open access archive for the deposit and dissemination of scientific research documents, whether they are published or not. The documents may come from teaching and research institutions in France or abroad, or from public or private research centers.

L'archive ouverte pluridisciplinaire **HAL**, est destinée au dépôt et à la diffusion de documents scientifiques de niveau recherche, publiés ou non, émanant des établissements d'enseignement et de recherche français ou étrangers, des laboratoires publics ou privés.



Distributed under a Creative Commons Attribution - NonCommercial 4.0 International License

A sustainable Fungal Microbial Fuel Cell (FMFC) for the bioremediation of acetaminophen (APAP) and its main by-product (PAP) and energy production from biomass

M. Pontié^{a*}, E. Jaspard^b, C. Friand^a, J. Kilani^a, A. Fix-Tailler^a, C. Innocent^c, D. Chery^d,
S. F. Mbokou^e, A. Somrani^{a,f}, B. Cagnon^g, P.Y. Pontalier^h

^a UBL Universities, University of Angers, Laboratory GEIHP EA 3142, Institut de Biologie en Santé, PBH-IRIS, CHU, 4 Rue Larrey, 49933 Angers Cedex 9, France

^b UBL Universities, University of Angers, Department of Biology, 2, Bd Lavoisier, 49045 Angers Cedex, France

^c Institut Européen des Membranes, UMR 5635, ENSCM-UMII-CNRS, Place Eugène Bataillon, 34095 Montpellier, France

^d Lycée polyvalent Bertène Juminer, 81 route saint Maurice 97320 Saint Laurent du Maroni, French Guyana, France

^e Electrochemistry and Chemistry of Materials, Department of Chemistry, University of Dschang, P.O. Box 67 Dschang, Cameroon

^f Al Jouf University, College of Sciences and Arts, Physics Sciences Department, Tabarjal, Kingdom of Saudi Arabia

^g ICMN Interfaces, Confinement, Matériaux et Nanostructures, UMR7374 - Université d'Orléans-CNRS, 1b rue de la Férollerie, 45071 Orléans Cedex 2, France

^h Toulouse University, INP-ENSIACET, LCA (Laboratory of Agro-industrial Chemistry), 31030 Toulouse France

* Correspondence: maxime.pontie@univ-angers.fr; Tel.: +33 666920935

ABSTRACT: A fungal biofilm of *Scedosporium dehoogii* was successfully elaborated and used as a bio anode in a microbial fuel cell device. The cathode was a carbon felt electrochemically modified by electrodeposition of a film of poly-Ni(II) tetrasulphonated phthalocyanine (poly-NiTSPc). The elaborated biofilm, formed by electrodeposition of a suspension of *Scedosporium dehoogii* worked to catalyze acetaminophen (APAP) oxidation in the anode. The optimal potential during the electrodeposition process was found to be 0.8 V *vs.* saturated calomel electrode (SCE) with a thickness of 3.5±0.2 µm. The fabricated fungal microbial fuel cell (FMFC) proved to be an efficient fuel in acetaminophen with highly stable output performances offering a power density of 50 mW m⁻² under an electromotive force of +550 mV in physiological conditions. The biodegradation of PAP, the main APAP by-product from bacterial biodegradation, was also studied and the optimal resistance from the usual polarization curves was 3.000 Ohm. Finally, the biodegradation of ligno-cellulosic materials such as bagasse, rapeseed, cellulose and lignin by *Scedosporium dehoogii* was successfully tested in Petri dishes. The growth of the fungus using these biomaterials as substrates followed the order: bagasse > rapeseed > cellulose > lignin. The FMFC was tested in the presence of natural lignin from sugarcane bagasse and complete degradation of the lignin by *S. dehoogii* biofilm was achieved with a power density of 16 mW m⁻².

Keywords: fungal microbial fuel cell; *S. dehoogii*; APAP/PAP/biomass; lignin; SEM/AFM

46

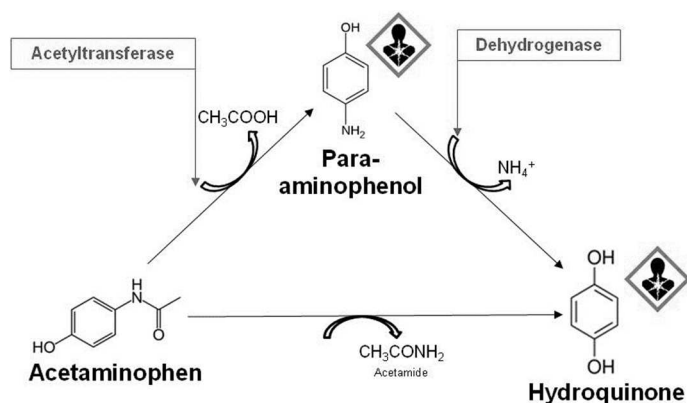
47 1. Introduction

48 The first recorded occurrence of electrochemical activity between bacterial/fungal (yeast)
49 species and electrodes can be traced back to the early 20th century. It was reported by Potter, 1911,
50 cultures of *Escherichia coli* and *Saccharomyces spp.* produced electricity using platinum
51 macroelectrodes in a battery type setup with sterile media. The story of electromicrobiology gained
52 new interest in 1963, when a NASA space program demonstrated the possibility of recycling and
53 converting human waste to electricity during space flights. In 1991, pioneering work by Habermann
54 and Pommer reported the long-term use of municipal wastewater by a microbial fuel cell (MFC)
55 without malfunction or maintenance. Moreover, this study reported indirect electron transfer (a
56 mechanism of electron transfer allowing specific bacteria to donate electrons) *via* soluble mediators.
57 In 1999, it was discovered that mediators were not essential components within MFC configurations,
58 thus allowing MFCs to be developed without the need for expensive mediators (see the review by
59 Slate *et al.*, 2019).

60 Since 2002 (Bergel and Féron, 2002), the performances of MFCs have quickly grown and leveled
61 off in 2008 respectively at a few W m⁻² in laboratory conditions, and at a few mW m⁻² in natural
62 environments, for a geometrical surface electrode (de Dios *et al.*, 2013). This stimulated increasing
63 interest in electromicrobiology research, which now boasts over a thousand energy-generation-cells
64 reported in the literature (Rahimnejad *et al.*, 2016; Ghasemi *et al.*, 2013). The first commercial
65 prototypes are expected soon (Slate *et al.*, 2019).

66 Concerning filamentous fungi, the most intensively studied systems are yeast-based MFCs,
67 where direct electron transfer via cytochrome *c* was reported (Hubenova and Mitov, 2015).
68 However, recent findings indicate that other fungi also have redox-active enzymes capable of
69 electrogenic activity in MFC systems (Morath *et al.*, 2012; Rahimnejad *et al.*, 2015). Fungi belonging to
70 the group of white-rot (well-known pharmaceuticals (Marco-Urrea *et al.*, 2009) and wood degraders)
71 were found to have an extracellular oxidative ligninolytic enzymatic system that enables them to
72 degrade lignin (Pollegioni *et al.*, 2015). The enzymes of this system can also degrade various
73 xenobiotic compounds and dyes (Sekrecka-Belniak and Toczyłowska-Maminska, 2018).

74 Research focusing on energy gain often needed to study their environmental impact (zero
75 waste). Indeed, the presence in treated wastewater of aromatic drug molecules such as diclofenac,
76 ibuprofen, paracetamol or carbamazepine (Langenhoff *et al.*, 2013) and their aromatic by-products
77 (p-aminophenol, hydroquinone...) demonstrates the inefficiency of bacterial treatments of these
78 molecules in conventional wastewater treatment units (Mashkour, *et al.* 2016). All of these molecules
79 may present a carcinogenic, mutagenic and reprotoxic (CMR) hazard, as illustrated in Figure 1 for
80 APAP.



81

82 **Figure 1.** Illustration of 2 degradation pathways of acetaminophen by bacteria (from Zhang *et al.*,

83 2013).

84 Many polycyclic aromatic hydrocarbons (PAHs) are also CMR compounds that can be
 85 degraded by several fungal enzymes (Kadri *et al.*, 2017).

86 *Scedosporium dehoogii* is a filamentous fungus belonging to a complex of five fungi strains
 87 named *Scedosporium apiospermum* (Gilgado *et al.*, 2008), living in soil (Alvarez and Sanhueza, 2016)
 88 and able to use aliphatic and aromatic hydrocarbons as carbon and energy sources: it can therefore
 89 be a good candidate for bioremediation purposes (Blasi *et al.*, 2016). This microorganism is mainly
 90 found in polluted waters and contaminated soils (sewage sludge, stagnant water ...). Although there
 91 are few data about the ecology of this filamentous fungus, it is known that its ecological
 92 environment is strongly impacted by human activities and this is true for almost all fungi (Harms *et al.*,
 93 2011). This was shown through its ability to metabolize hydrocarbons (especially aromatics) as a
 94 source of carbon and energy (Blasi *et al.*, 2016). This filamentous fungus is a model of bio-indicators
 95 for anthropogenic pollution, and also a microorganism of choice for bioremediation, as recently
 96 reported (Sekrecka-Belniak and Toczyłowska-Maminska 2018).

97 As a typical example, Mbokou *et al.* (2016a) demonstrated that the biodegradation of APAP by
 98 *S. dehoogii* does not lead to the formation of either *p*-aminophenol (PAP) or hydroquinone (HQ).
 99 Moreover, the first *S. dehoogii*-based MFC using APAP as fuel was recently developed with a power
 100 density of 6.5 mW/m² (Mbokou *et al.*, 2017).

101 The power density obtained for various fungi/yeast MFCs is presented in Table 1.

102 **Table 1.** Examples of some fungi-/yeast-based MFC performances.

Micro-organism	Electron donor	Power density (mW m ⁻²)	Reference
<i>Saccharomyces cerevisiae</i>	glucose	155	(Bennetto <i>et al.</i> , (1983))
<i>Saccharomyces cerevisiae</i>	synthetic wastewater	283	(Raghavulu <i>et al.</i> , (2011))
<i>Saccharomyces cerevisiae</i>	glucose	344	(Christwardana <i>et al.</i> (2017))
<i>Arxula adenivorans</i>	dextrose and glucose	28	(Haslett <i>et al.</i> , (2011))
<i>Candida melibiosica</i>	various carbohydrates	60	(Hubenova and Mitov (2010))
<i>Candida sp.</i>	glucose from wastewater	21	(Lee <i>et al.</i> , 2015)
<i>Hansenula anomala</i>	various carbohydrates	690 - 2900	(Prasad <i>et al.</i> , 2007)
<i>Scedosporium dehoogii</i>	APAP	6.5	(Mbokou <i>et al.</i> , 2017)
<i>Scedosporium dehoogii</i>	APAP	50	This work
<i>Scedosporium dehoogii</i>	Lignin	16	This work

103
 104 The present paper reports the results of an investigation into the potential bioremediation of
 105 para-aminophenol (PAP) from wastewater and energy production in an MFC comprising an *S.*
 106 *dehoogii* carbon felt anode. The oxidation of APAP and energy production were studied. The
 107 feasibility of the biodegradability of PAP by *S. dehoogii* was also explored. Finally, the
 108 biodegradability of several ligno-cellulosic materials (bagasse, rapeseed, cellulose, lignin) by *S.*
 109 *dehoogii* was studied in Petri dishes and the natural lignin from sugarcane bagasse was tested for the
 110 first time as fuel in a FMFC.

111 2. Experimental

112 2.1. Reagents

113 APAP was purchased from Sigma-Aldrich. A 0.1 M phosphate buffer solution (PBS) of pH 7.4
 114 was used as supporting electrolyte. All other aqueous solutions were prepared from analytical grade
 115 chemicals and deionized water with a pH of 6.5, conductivity < 1 µS cm⁻¹ and TOC < 0.1 mg L⁻¹ (Elga
 116 Lab Water ultrapure-water system, Purelab-UV-UF, Elga).

117 2.2. Apparatus and electrochemical measurements

118 All the electrochemical experiments were performed using a PG580 analyzer (Uniscan
119 Instruments, UK). The electrochemical software used was UiEchem version 3.27 (Uniscan
120 Instruments, Biologic company, France). A conventional three-electrode cell configuration was
121 employed. Working electrodes (0.071 cm² of geometric area) as recently published (Prasad et al.,
122 2007) consisted in carbon paste electrodes (CPE) modified by cellulose fibers. The reference electrode
123 was a saturated calomel electrode (SCE). Platinum wire (10 cm length and 4 mm diameter) and grid
124 (1 cm of diameter) were respectively used as the counter electrodes for
125 APAP/PAP/4-hydroxybenzoate (4-HBz) analysis by CPE and biofilm polarization/cathode
126 modification. An aqueous sample was taken once daily from the anode compartment. The residual
127 concentration of APAP was electrochemically determined using square wave voltammetry (SWV)
128 on our homemade modified CPE. For APAP and PAP analyses, the SWV optimized parameters
129 were a frequency of 400 Hz, pulse height of 90 mV, scan increment of 15 mV and initial potential of
130 -0.2 V vs. SCE.

131 2.3. Strains and Materials

132 Four *S. dehoogii* strains UA 110350859-01, 110350889-01, 110354504-01 and 110350150-01,
133 isolated from soil samples in the vicinity of Angers (France) were used throughout this study in
134 order to find the best strain to use in the MFC device. The fungi were routinely maintained by
135 weekly passages on a yeast extract-peptone-dextrose (YPD) agar medium containing in g L⁻¹: yeast
136 extract, 5 g; peptone, 5 g; dextrose, 20 g and chloramphenicol, 0.5 g. The ability of *Scedosporium*
137 strains to use APAP, PAP, HQ and 4-hydroxybenzoate (4-HBz) as the sole carbon source was
138 investigated by cultivating the fungi on Scedo-Select III agar plates (Pham et al., 2015) containing
139 each molecule respectively, as follows. Conidia were harvested from 1-week-old cultures at 25-30°C
140 on YPD medium plates by flooding the agar surface with 15 mL of ultrapure water. The fungal
141 suspension was then filtrated on a 40 µm pore size sterile nylon filter and conidia were pelleted by
142 centrifugation at 4000 g (5 min at 4°C). They were resuspended in 10 mL of sterile ultrapure water,
143 and finally enumerated using a hemocytometer. Conidia were then inoculated onto Scedo-Select III
144 agar plates containing either APAP, 4-HBz, PAP or HQ, as carbon sources. For this purpose, stock
145 solutions of these pharmaceuticals (1 g each in 100 mL of ultrapure water) were prepared and
146 sterilized by filtration (0.2 µm pore size sterile membrane). After addition of the carbon source to the
147 culture medium at a final concentration of 0.9 g L⁻¹ and inoculation with conidia of *S. dehoogii* (10⁴ in
148 10 µL), the plates were incubated during 1 week at 25°C. Growth of the fungus was followed by
149 measuring the diameter of the mycelium on the plate every day for 1 week (see Table 2 in the results
150 and discussion section).

151 Biofilm formation by *S. dehoogii* was obtained by two successive subcultures on the same
152 medium containing 4-HBz instead of glucose. After two weeks of incubation, conidia were
153 harvested from cultures on YPD plates by flooding the agar surface with 15 mL of ultrapure water.
154 The suspension was then filtrated on a 40 µm pore size sterile nylon filter and conidia were pelleted
155 by centrifugation at 4000 g for 5 min at 4°C. They were resuspended in 10 mL of sterile ultrapure
156 water. Finally, a suspension of roughly 10⁶ spores mL⁻¹ was used for the formation of the biofilm on
157 carbon felt.

158 2.4. Bioanode elaboration

159 Carbon Felt (CF) (Carbon Lorraine supplier, France) (CF geometrical area = 10 cm²) was used as
160 the substrate for fungal biofouling deposition. Prior to use, the CF was cleaned successively using a 1
161 M HCl solution and ultrapure water. Following the usual practice, the CF was then immersed in a
162 1:1 (volume ratio) mixture of ethanol-water for a few minutes followed by sonication 2 min. (47 kHz)
163 in ultrapure water to achieve ethanol rinsing. The CF was finally autoclaved at 120°C during 15 min.
164 before colonization by the fungus.

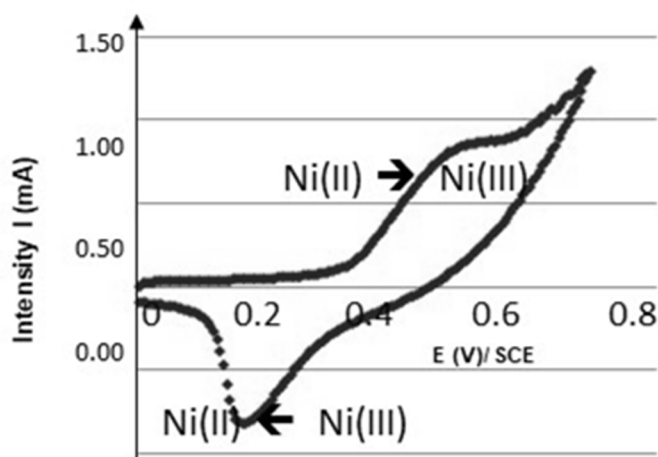
165 The CF anode was immersed in a suspension of *S. dehoogii*. The biofilm was then developed by
166 polarization of the CF at -0.15 V *vs.* SCE during one week under sterilized conditions (laminar oven)
167 (Figure S2, Supplementary Information). The sole source of carbon was 4-HBz at 0.9 g L⁻¹ for the
168 formation of the biofilm. As illustrated in Figure S2, above 90% of the 4-HBz was consumed after 7
169 days. The initial current density at the potential -0.15 V *vs* SCE was 175 mA m⁻² at t=0 and after 1
170 week attained the value of 375 mA m⁻². The potentiostat used was an electrochemical analyzer VASD
171 40, connected to a three-electrode system. Carbon felt, SCE and a platinum wire were the working
172 electrode, the reference electrode and the counter electrode, respectively. The homemade
173 cellulose-based CPE was used to follow the consumption of 4-HBz.

174 2.5. Preparation of CPE

175 The CPE was prepared by thoroughly hand mixing 5 mg of cellulose fibers, 30 mg of silicone oil
176 and 65 mg of graphite powder (analytical grade, ultra F, < 325 mesh, from Alfa) in a mortar, as
177 described elsewhere (Pontie *et al.*, 2017). A portion of the composite mixture was packed into the
178 cylindrical hole of a Teflon[®] tube equipped with a copper wire serving as electrical contact to
179 maintain contact for electrochemical measurements. The surface exposed to the solution was
180 polished on a weighing paper to give a smooth aspect before use.

181 2.6. Cathode elaboration

182 The CF cathode was first electrochemically pretreated under the following conditions: CV
183 between 0.0 and 1.2 V *vs.* SCE in 0.1 M NaOH during 10 cycles (scan rate 0.1 V s⁻¹). CF pretreatment
184 is essential to achieve good reproducibility of the poly-NiTSPc film deposition. The electrochemical
185 deposition of poly-NiTSPc was achieved in 0.1 M NaOH and 2 mM NiTSPc aqueous solution at a
186 fixed potential of +0.8 V *vs.* SCE during 3000 s in order to optimize the poly-NiTSPc matter to be
187 deposited. The effect of poly-NiTSPc electrodeposited on a carbon felt surface has been studied
188 previously (Champavert *et al.*, 2015). Although the electrocatalytic effect of this film on oxygen
189 reduction has not been demonstrated, the presence of the poly-NiTSPc film was useful to reach a
190 larger surface area. In this study, preparation of the poly-NiTSPc film was optimized in terms of its
191 electrodeposition potential.



192

193 **Figure 2.** Cyclic voltammetry of CF/poly-NiTSPc cathode in NaOH 0.1 M.

194 We then optimized the electrodeposition potential between 0.4 V and 1.2 V (results not shown).
195 No film was observed below 0.6 V and over 1.0 V due to overlap between water oxidation and film
196 electrodeposition. The optimum potential observed was 0.8 V *vs.* SCE. The thickness of the
197 electrodeposited film was estimated at 3.5±0.2 μm from Faraday's law.

198 The CF zeta potential was measured with a commercialized zetameter apparatus (surPASS3,
199 Anton Paar Company, Austria). The measures were carried out with KCl 10⁻⁴ M and pH 6.5, for
200 unmodified and modified poly-NiTSPc CF. A zeta potential of -25 mV was obtained for the
201 unmodified as in presence of poly-NiTSPc film the zeta potential value decreased to -49 mV, proving
202 the electrodeposition of poly-NiTSPc on CF, as also proved by the redox system Ni(III)/Ni(II)
203 observed in Figure 2.

204 2.7. Fungal Microbial biofuel cell set up

205 The FMFC set up was divided into two compartments, as recently reported (Mbokou *et al.*,
206 2017). The compartments were separated by a Nafion 117[®] membrane which allows protons to cross
207 it from the anode to the cathode chamber. The anode chamber solution consisted of 100 mg L⁻¹ APAP
208 in 0.1 M phosphate buffer solution (PBS), pH 7.4. Nafion 117 samples were conditioned in a fridge (4
209 °C) in NaCl aqueous solution at a concentration of 1 M and fully rinsed with ultrapure water before
210 use in the FMFC.

211 The solution of the cathode chamber was also PBS. O₂ from air was provided to the cathode
212 chamber before filtration using a 0.45 µm filter. An external resistance of 1 kΩ was connected to the
213 electrodes in order to shuttle electrons from anode to cathode. This external resistance was used to
214 determine the power output during MFC discharge. The MFC started to function when APAP (100
215 mg L⁻¹) was added in the anode compartment. Residual APAP concentrations in this compartment
216 were measured daily using the SWV technique on the CPE as described above (see section 2.5). All
217 our experiments were carried out at room temperature. In open circuit the electromotive force was
218 measured at +550 mV. During the experiments measuring the power density we estimated that the
219 internal resistance of the MFC was around 5000 Ohm. Furthermore, as an initial control we did not
220 observe any power density in the absence of APAP (or lignin).

221 222 2.8 TOC and phenolic compounds (polymeric and monomeric) analyzed in the FMFC

223 Total organic carbon (TOC) was measured for the experiments conducted in the presence of APAP
224 as the carbon source. The fractional removal of TOC was estimated by measuring the TOC with a
225 TOC-meter-LCSH FA (Shimadzu). TOC was deduced from the values of total carbon (TC) and
226 inorganic carbon (IC). The mobile phase was an acetonitrile/water mixture introduced at a flowrate
227 of 0.8 mL min⁻¹ with a 5-80% gradient.

228 In the case of Lignin as the carbon source in the FMFC, the phenolic composition of the medium was
229 analyzed before and after the experiment according to the Folin-Ciocalteu method with 96-well
230 microplates. Each well was fed 20 µL of sample, then 10µL of commercial Folin-Ciocalteu reagent
231 and 170 µL of Na₂CO₃ alkaline solution at 2.36% were added. The optical density was read after 45
232 minutes of reaction at 700 nm with a specific plate reader (BMG-Labtech Spectrostar-Nano). This
233 colorimetric method was used with a calibration curve obtained with different concentrations of
234 gallic acid. The total concentration in phenolic compounds is therefore given in gallic acid
235 equivalent.

236 The phenolic monomer composition of the medium was characterized by HPLC on an OmniSpher 3
237 C18 100 x 4.6 column (Agilent Technologies). The gradient was as follows: 91% acidified water (1%
238 acetic acid (v/v)) and 9% acetonitrile for 25 min, from 9 to 90% acetonitrile in 5 min, kept constant for
239 5 min, then decreased back to 91% acidified water in 5 min; the column was equilibrated for 7 min
240 between runs. The flow rate was 0.5 mL/min, the injection volume was 10 µL and the column
241 temperature was maintained at 25 °C. The UV detector was set at 280 nm. Concentrations for the
242 calibration curves ranged between 0 and 200 mg/L. Standard and process samples were diluted in
243 acetonitrile: water at a ratio of 50:50 (v/v) prior to injection. Gallic acid, 4-hydroxybenzoic acid,
244 caffeic acid, syringic acid, vanillic acid (VA), 4-hydroxybenzaldehyde (4HBA), vanillin, *p*-coumaric

245 acid (*p*-CA), syringaldehyde, ferulic acid (FA), sinapic acid and hydroxycinnamic acid were
246 quantified.

247 2.9. Field emission gun scanning electron microscopy (FEGSEM) and atomic force microscopy (AFM) 248 characterizations

249 The FEGSEM equipment used was a LEO 1530 apparatus (SCIAM, Angers University, France)
250 at a 3 keV acceleration voltage to minimize the irradiation damage and obtain a resolution of a few
251 nanometers. The topography 3SD image of the biofilm deposited on the CF was obtained using an
252 Atomic Force Microscopy set-up (Nanoscope III from Bruker, Germany). Samples were attached to
253 steel discs and were then recovered by an ultra-thin layer of Pt (4 nm) deposited by evaporation
254 under vacuum (BAL-TEC MED 020 Balzers Lichtenstein apparatus) for FEGSEM observations.

255 2.10. Ligno-cellulosic matter

256 Bagasse from sugar cane and lignin were provided by the laboratory LCA (Toulouse,
257 ENSIACET, France). Rapeseed was obtained from ICMN (Orleans, France). Cellulose powder was
258 purchased from Fluka Company. Growth of *S. dehoogii* was followed by measuring the diameter of
259 the mycelium on the plate daily during 1 week, as detailed in section 2.3.

260 3. Results and discussion

261 3.1. Comparison of the growth of different *S. dehoogii* strains in the presence of different aromatic molecules

262 We compared the radial diameter growth (Figure S1A) on agar plates of four strains of *S.*
263 *dehoogii* in the presence of different carbon sources by measuring the diameter of the mycelium
264 during one week (Table 2).

265 **Table 2.** Radial diameter (in mm) of the mycelium of 4 strains of *S. dehoogii* grown on
266 different carbon sources at 25°C.

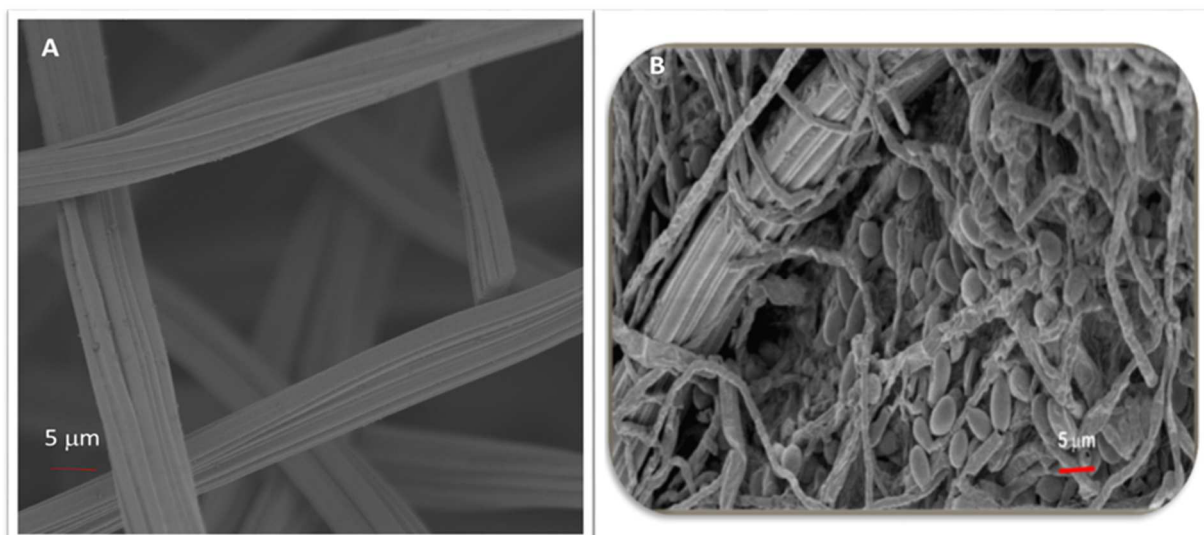
Strains	Source of carbon			
	4-HBz	APAP	HQ	PAP
110350150-01 (1)	21	15	14	14
110354504-01 (2)	18	15	12	14
110350859-01 (3)	20	15	9	11
110350889-01 (4)	17	17	10	7

267 Strain 1 appeared to be the most effective in metabolizing APAP and its degradation
268 by-products (PAP and HQ), with 4-HBz as the reference. Based on these results, we chose strain
269 110350150-01(1) for the rest of the experiments.

270 3.2. Morphological and topographical characterizations of the fungal bioanode

271 The surface morphology of the carbon felt was observed (Figure 3) using FEGSEM apparatus.
272 This revealed the formation of a biofilm.

273
274

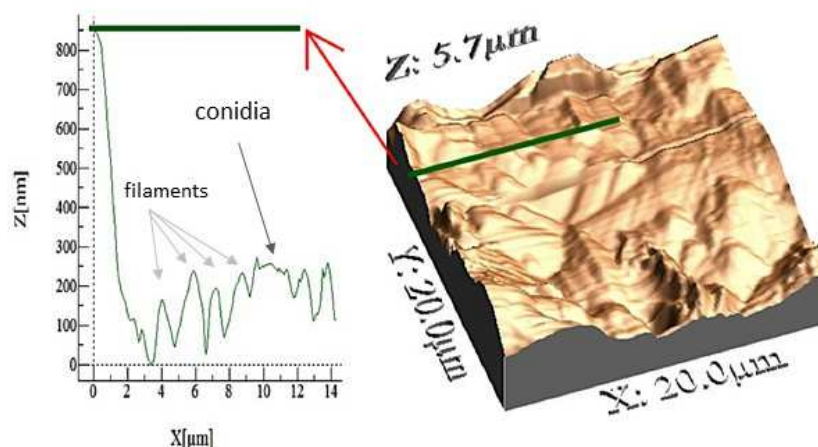


275
276
277

Figure 3. 2D-FEG-SEM image of unmodified carbon felt (A) and carbon felt covered by a biofilm of *Scedosporium dehoogii* after polarization during 7 days (B).

278 After 1 week of polarization, conidia and filaments of the fungus became visible (center - right
279 of Figure 3). A CF fiber of 12 μm diameter was observed top left.

280 To complete FEGSEM observations, the topographical characterization of the biofilm was
281 drawn in 3D (Figure 4). A zoom on the green line in Figure 7 enabled measurement of the diameter
282 of the filaments (around 2 μm) and that of conidia (around 5 μm).



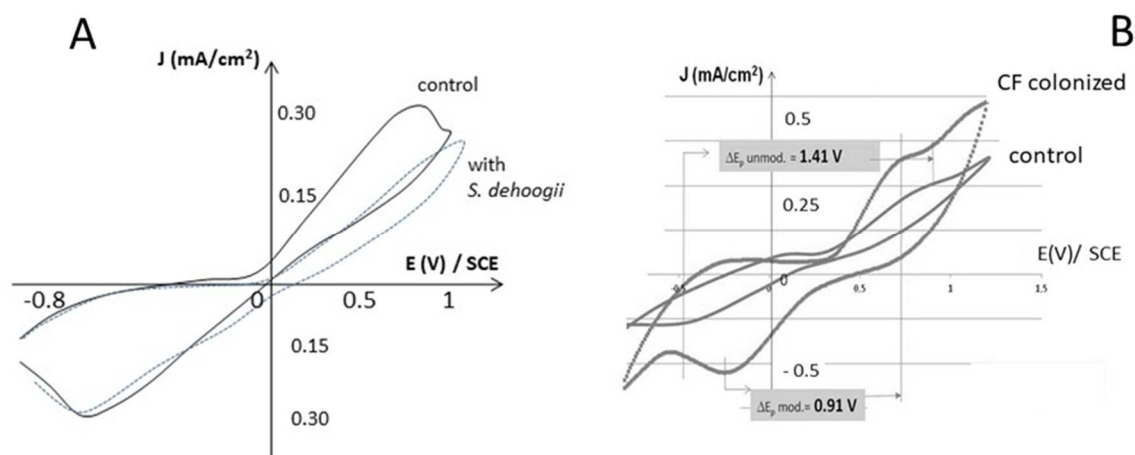
283
284

Figure 4. AFM 3D-image of the *S. dehoogii* biofilm developed on the carbon felt.

285 Figures 3 and 4 are complementary illustrations of the presence of the *S. dehoogii* biofilm on the
286 CF anode (see also Figure S2B for a macroscopic view of the bioanode).

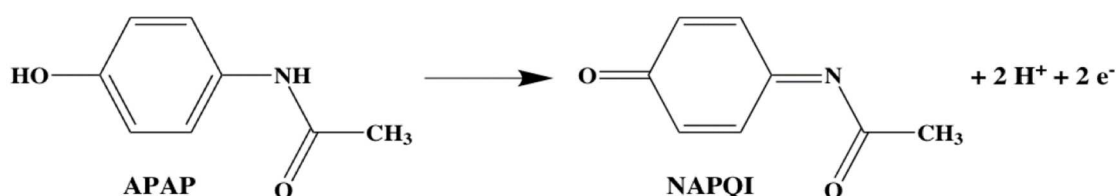
287 3.3. Proving the connection of *S. dehoogii* to CF

288 One of the technological barriers often encountered by bioelectrochemists is the connection of
289 the microorganisms to the electrodes, which does not necessarily operate directly. We studied the
290 kinetics of electron transfer for the redox system NAPQI/APAP (NAPQI, N-acetyl-*p*-benzoquinone
291 imine scheme 1) in order to compare the unmodified CF (control, Figure 5) and that covered by the
292 *S. dehoogii* biofilm (CF colonized by *S. dehoogii*).



293
294
295
296

Figure 5. Cyclic voltammograms of the carbon felt colonized or not, at a scanning rate of 200 mV s⁻¹, in the presence of APAP 50 mg L⁻¹ in PBS : **(A)** Non-colonized CF (control) without and with a suspension of *S. dehoogii*; **(B)** CF colonized or not (control) by *S. dehoogii*



297
298

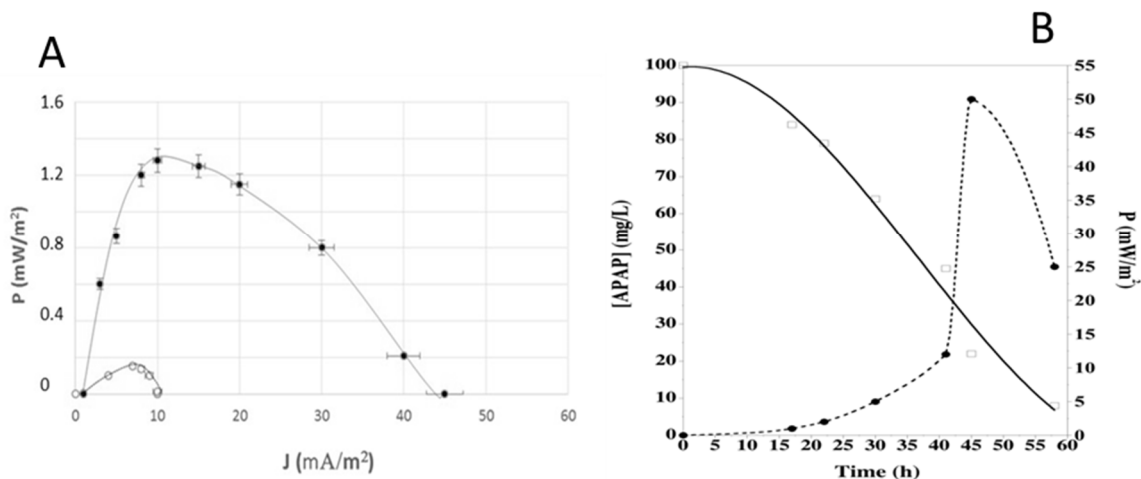
Scheme 1. Electrochemical oxidation of APAP.

299 Figure 5 shows that in the case of the NAPQI/APAP redox system (scheme 1), the kinetics of
300 electron transfer of *Scedosporium dehoogii* coated CF is faster than that on the unmodified one: a
301 decrement of 500 mV in ΔE_p was observed with the biofilm vs no biofilm (see Fig. 5B). At the same
302 time, the current density of the APAP oxidation signal on the colonized CF increased by a factor of
303 2.5. These results demonstrate the ability of the *S. dehoogii* biofilm to electrocatalyze the oxidation of
304 APAP.

305 It shows for the first time a good connection between the fungus *S. dehoogii* and the anode
306 material. It remains to be elucidated whether it is an external enzyme or an internal process that is
307 involved in this connection.

308 3.4. FMFC performances

309 The electrons generated by *S. dehoogii* from APAP are directly transferred to the anode. Then,
310 they flow to the cathode through a conductive material containing a resistor. Electrons reaching the
311 cathode combine with protons diffusing from the anode through the proton exchange and oxygen
312 provided by air, thereby resulting in the formation of water. When electrons flow from the anode to
313 the cathode, they generate current and voltage to make direct energy. Figure 6 shows the
314 degradation kinetics of APAP along with the power density generated by the MFC.



315
316
317

Figure 6. : (A) Evolution of the power density *vs.* current density; (B) Kinetic of APAP concentration and power density in the fungal MFC. Legend: ●with biofilm; ○ without biofilm

318
319
320
321
322
323

Figure 6A shows the polarization curves of the FMFC without and with biofilm. In both cases an optimal resistance was obtained and found to be around 3 000 Ohm at the maximum power density. In Figure 6B, the APAP concentration started to decrease along with the growth of the fungal biofilm on the anode. This means that APAP has been degraded by fungi and used as a carbon and energy source.

324
325
326
327
328

The power density delivered by the FMFC increased gradually after APAP addition, indicating the absence of a transitory state (no adaptation period) of *S. dehoogii* (*i.e.*, the biofilm) to the drug. After roughly 40 h, the power density increased to a maximum value of 50 mW m⁻² while at the same time the APAP concentration decreased. So we observed as elsewhere that APAP decreases when the power decreases.

329
330
331
332

The shape of the curve is identical to that obtained for the degradation kinetic of another pharmaceutical (*i.e.*, naproxen) by the fungus *Phanerochaete chrysosporium*: degradation percentages were 9% and 83% after 2h and 23 h of fungus action, respectively (Rodarte-Morales *et al.*, 2012).

333
334
335

Furthermore, TOC measured after 7 days in the anode compartment was found to be 22 mg/L when the initial APAP concentration was 100 mg/L. No by-products such as PAP or HQ were detected (results not shown).

336
337

Then, under the hypothesis of a complete combustion of APAP, the fuel cell reaction can be written:

338



339

Scheme 2. APAP combustion reaction (hypothetical) in the FMFC

340
341
342

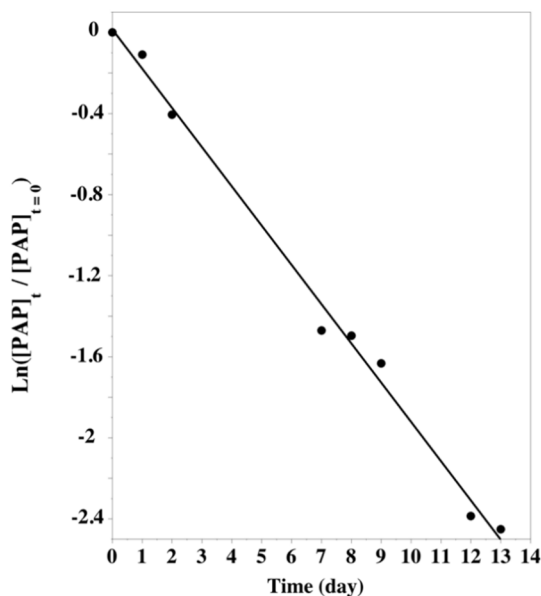
Then, in a the complete combustion of APAP 37 e- per mol. are delivered as in the case of glucose only 24 e- are released.

343
344
345
346
347
348
349

Comparing our results with those reported in Table 1, we can observe a higher power density than that found by other authors. This can be attributed to the fact that the biofilm was developed only at the external surface for the CF electrode. In the present work, however, the power density was improved (Champavert *et al.*, 2015) by optimizing the electrodeposition of phthalocyanine dedicated to the oxygen reduction reaction.

350 3.5. PAP biodegradation studies

351 The consumption of PAP by *Scedosporium dehoogii* was monitored by our homemade CPE
352 (Figure 7).



353

354

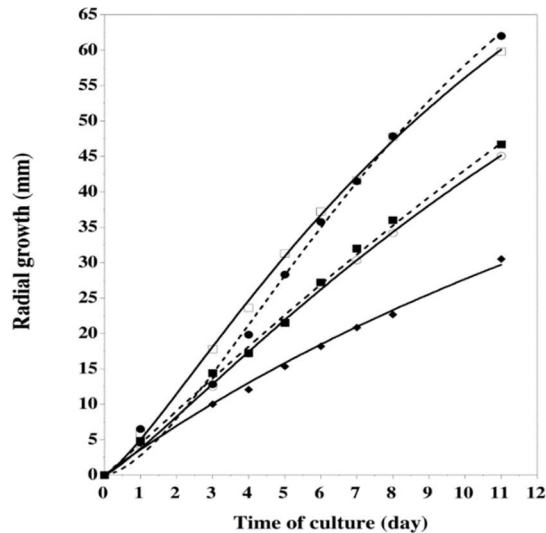
Figure 7. Kinetic of the biodegradation of PAP by *S. dehoogii* at 25°C.

355 This confirmed the results reported in Table 2, showing that *S. dehoogii* is able to use PAP as a
356 source of carbon in Erlenmeyer flasks. The kinetic follows a process of pseudo-order 1 with a kinetic
357 constant of 0.19 day⁻¹, and a half-life of 3.3 days. This results are closer to those obtained by Mbokou
358 (Mbokou *et al.*, 2017) for APAP biodegradation in the same FMFC set-up, where a kinetic constant of
359 0.11 day⁻¹ and half-life of 6.3 days were found.

360 3.6. Plant biomass as the source of carbon for *Scedosporium dehoogii*

361 Wastewaters usually contain very low concentrations of pharmaceutical compounds (a
362 few $\mu\text{mol L}^{-1}$ or less) and cannot allow our FMFC to attain a very high power density. Therefore, we
363 decided to test a cellulose-based source of carbon from ligno-cellulosic materials (LCM) as a new
364 source of fuel. LCM is mainly composed of cellulose, hemi-cellulose and lignin. They constitute the
365 most important source of organic carbon on earth and account for nearly all carbon sequestered
366 annually in plant matter (Mbokou *et al.*, 2016b). Lignins are complex nonlinear polymers, whose
367 precursor is phenylalanine (Davin *et al.*, 2008). In particular, lignins are a major source of aromatic
368 carbon on Earth, where it accounts for nearly 30% of carbon sequestered in plant biomass. There is a
369 great diversity of lignins. Plant polymers thus constitute very abundant energy sources whose
370 bioremediation reduces their carbon footprint. Numerous fungi are known to degrade LCM (for
371 example, *Scedosporium apiospermum*, *Pleurotus ostreatus*, *Phanerochaete chrysosporium* ...) because they
372 possess lignin-modifying enzymes (Morales *et al.*, 2017).

373 Figure 8 shows the growth of *S. dehoogii* in a Petri dish with PDA as substrate in the presence of
374 different plant biomasses: bagasse, rapeseed, cellulose and lignin.



375

376 **Figure 8.** Radial growth on different carbon sources: (●) bagasse; (□) rapeseed, (○) cellulose, (◆)
 377 lignin, (■) PDA, potato dextran agar, is the reference).

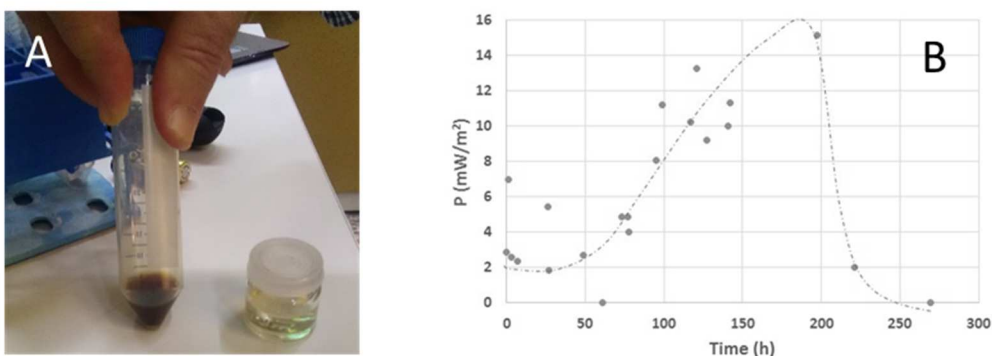
378 The results show for the first time that *Scodosporium dehoogii* can metabolize different plant
 379 biomasses as a source of carbon and energy. As shown in figure 8, the rate of growth of the fungus
 380 decreased following the order: bagasse - rapeseed > cellulose > lignin.

381 Based on these encouraging results, we explored the feasibility of lignin as biofuel in our FMFC.
 382 In fact, lignocellulosic or second biorefineries transform agricultural by-products or forest
 383 biomass into energy (i.e. thermal), various chemicals and also materials (Oriez *et al.* 2019).

384 In the last part of our work, we therefore tested for the first time the biodegradability of
 385 sugarcane bagasse lignin in our FMFC device.

386 3.7. FMFC performances with lignin

387 The fabricated FMFC started functioning when lignin 1 g.L⁻¹ (first injection) was introduced into the
 388 anode compartment.



389

390 **Figure 9.** A- Lignin alkaline solution (brown color) (day 0 in the FMFC) and lignin decolorized
 391 (day 10 in the FMFC); B- Power density vs time in presence of lignin as source of C

392

393 Residual lignin species such as monolignols were not detected after 10 days residence time in the
 394 anode compartment of the FMFC. A decolorization was observed as illustrated in Figure 9A. The
 395 analysis of the medium with lignin showed that it had an initial concentration of 1.84 g GAE (Gallic
 396 acid equivalent)/L. At the end of the experiment, the concentration was only 0.24 g GAE/L, meaning

397 that 87% of the lignin had been removed. HPLC analysis did not show any monomeric compounds,
398 indicating that the degradation of lignin molecules was complete and did not lead to the production
399 of small molecules. It can be assumed that lignin was used as the source of carbon and completely
400 degraded by the strain, which can explain the sharp decrease in the electric production, after 200 h,
401 due to the lack of the carbon source.

402 The power density generated by the FMFC in the presence of lignin as a function of time was
403 monitored, as illustrated in Figure 9B. It shows a maximum power density of 16 mW/m² for a time
404 of 200h.
405

406 4. Conclusions and perspectives

407 It has been demonstrated for the first time that a biofilm of *Scedosporium dehoogii* developed by
408 polarization at -0.15 V vs. SCE during one week established a connection to a CF bioanode. The
409 cathode of our fungal MFC presented an optimum potential of 0.8 V vs. SCE for 3.5±0.2 μm thickness
410 of poly-NiTSPc film. We have also shown that APAP is an efficient fuel for this FMFC. Stable output
411 performances were obtained giving a power density of 50 mW m⁻² for an EMF of 550 mV.

412 Furthermore, the biodegradation of PAP, the main APAP by-product from bacterial
413 biodegradation was studied and *Scedosporium dehoogii* was able to use PAP as the sole source of
414 carbon and energy.

415 Lignocellulosic materials were tested for their ability to be potential carbon sources in the FMFC
416 device. The rate of growth of the fungus decreased following the order: bagasse ~ rapeseed >
417 cellulose > lignin.

418 The results obtained from the biodegradation of APAP, PAP and the plant materials by *Scedosporium*
419 *dehoogii* are promising and can be a way to valorize LCM in energy production. The power density
420 delivered by the fungal bioanode is considered better, a fact making *Scedosporium dehoogii* a great
421 alternative for the development of novel FMFCs with sustainable carbon sources.
422

423 In the near future, we will conduct first experiments with other fungi as *Scedosporium dehoogii*
424 because very recent results demonstrated its previously suspected pathogenicity for human beings.
425 The goal will be to achieve a better characterization of the enzymes involved in the degradation
426 processes and to increase the power density developed by our FMFC.
427

428 To conclude we have often observed biofouling on the surface of the Nafion[®] membrane on the side
429 in contact with the fungal biofilm, antifouling strategies should be developed and tested and/or
430 development of a new proton exchange membranes under low cost and dedicated to its application
431 in microbial fuel cells.
432

433 **Acknowledgments:** The authors wish to thank R. MALLET for recording FEGSEM/AFM images at the
434 microscopy department (SCIAM) of the University of Angers (France). We also thank the University of Angers
435 for funding allocated to Dr. Serge MBOKOU FOUKMENIOK for his 4-month internship in France. Many thanks
436 to Julia B. RAZAFIMANDIMBY for providing the strain of *Scedosporium dehoogii*. We are very thankful to the
437 LCA lab (ENSIACET, Toulouse, France) for providing the biomass. Thanks also to LE PALAIS DE LA
438 DECOUVERTE DE PARIS (France), especially to Romain ATTAL who gave us the opportunity to exhibit to the
439 public our work on FMFC during 2 months (Oct. 3rd to Nov. 25th 2018).

440

441

442

443 **References**

- 444 Alvarez, E., Sanhueza, C., 2016. New record of *Scedosporium dehoogii* from Chile: Phylogeny and susceptibility
445 profiles to classic and novel putative antifungal agents. *Rev. Iberoam. Micol.* 33, 224-229.
- 446
- 447 ATSDR, 2017. Agency for toxic substances and disease registry, U.S. Dep. Health Hum. Serv. USA.
448 <http://www.atsdr.cdc.gov/SPL/index.html>
- 449
- 450 Bennetto, H.P., Stirling, J.L., Tanaka, K., Vega, C.A., 1983. Anodic reactions in microbial fuel cells. *Biotechnol.*
451 *Bioeng.* 25, 559–568. DOI:10.1002/bit.260250219
- 452
- 453 Bergel, A., Féron, D., 2002. *French Patent* CNRS 6 August 2002, (FR 02/100009).
- 454
- 455 Blasi, B., Polynter, C., Rudavsky, T., 2016. Pathogenic yet environmentally friendly? Black fungal candidates for
456 bioremediation of pollutants. *Geomicrobiol J.* 33, 308-17 and references therein.
457 <https://www.tandfonline.com/doi/full/10.1080/01490451.2015.1052118>
- 458
- 459 Champavert, J., Ben Rejeb, S., Innocent, C., Pontié, M., 2015. Microbial fuel cell based on Ni-tetra sulfonated
460 phthalocyanine cathode and graphene modified bioanode. *J. Electroanal. Chem.* 757, 270-276.
461 <http://dx.doi.org/10.1016/j.jelechem.2015.09.012>
- 462
- 463 Christwardana, M., Kwon, Y., 2017. Yeast and carbon nanotube based biocatalyst developed by synergetic
464 effects of covalent bonding and hydrophobic interaction for performance enhancement of membraneless
465 microbial fuel cell. *Bioresour. Technol.* 225, 175–182. DOI: 10.1016/j.biortech.2016.11.051
- 466
- 467 Davin, L.B., Jourdes, M., Patten, A.M., Kim, K.W., Vassao, D.G., Lewis, N.G., 2008. Dissection of lignin
468 macromolecular configuration and assembly: comparison to related biochemical processes in allyl/propenyl
469 phenol and lignan biosynthesis. *Nat. Prod. Rep.* 25, 1015-1090.
- 470
- 471 de Dios M.A.F., del Campo A.G., Fernandez, F.J., Rodrigo, M., Pazos, M., Sanroman M.A., 2013. Bacterial–
472 fungal interactions enhance power generation in microbial fuel cells and drive dye decolorization by an ex situ
473 and in situ electro-Fenton process. *Bioresource Technology.* 148, 39-46.
- 474
- 475 Gilgado, F., Cano, J., Gené, J., Sutton, D.A., Guarro, J., 2008. Molecular and phenotypic data supporting distinct
476 species statuses for *Scedosporium apiospermum* and *Pseudallescheria boydii* and the proposed new species
477 *Scedosporium dehoogii*. *J Clin Microbiol.* 46, 766–771.
- 478
- 479 Habermann, W. and Pommer E –H, 1991, Biological fuel cell with sulphide storage capacity, *Appl.*
480 *Microbial Biotechnol.* 35, 128-133
- 481
- 482 Harms, H., Schlosser, D., Wick, L.Y., 2011. Untapped potential: exploiting fungi in bioremediation of hazardous
483 chemicals. *Nat. Rev. Microbiol.* 9, 177–192.
- 484

485 Haslett, N.D., Rawson, F.J., Barriere, F., Kunze, G., Pasco, N., Gooneratne, R., Baronian, K.H.R., 2011.
486 Characterization of yeast microbial fuel cell with the yeast *Arxula adenivorans* as the biocatalyst. *Biosens.*
487 *Bioelectron.* 26, 3742–3747. DOI:10.1016/j.bios.2011.02.011.
488
489 Hubenova, Y., Mitov, M., 2015. Extracellular Electron transfer in yeast-based biofuel cells: A review.
490 *Bioelectrochemistry.* 106, 177-185. doi.org/10.1016/j.bioelechem.2015.04.001
491
492 Hubenova, Y., Mitov, M., 2010. Potential application of *Candida melibiosica* in biofuel cells. *Bioelectrochemistry.*
493 78, 56–61. DOI:10.1016/j.bioelechem.2009.07.005
494
495 Kadri, T., Rouissi, T., Kaur Brar, S., Cledon, M., Sarma, S., Verma, M., 2017. Biodegradation of polycyclic
496 aromatic hydrocarbons (PAHs) by fungal enzymes: A review. *J. Environ. Sci.* 51, 52–74.
497
498 Langenhoff, A., Inderfurth, N., Veuskens, T., Schraa, G., Blokland, M., Kujawa-Roeleveld, K., Rijnaarts, H., 2013.
499 Microbial removal of the pharmaceutical compounds Ibuprofen and diclofenac from wastewater. *Biomed. Res.*
500 *Int.*, 2013, 325806
501
502 Lee, Y.-Y., Kim, T.G., Cho, K.-S., 2015. Isolation and characterization of a novel electricity-producing yeast,
503 *Candida sp.* IR11. *Bioresour. Technol.* 192, 556–563. DOI: 10.1016/j.biortech.2015.06.038
504
505 Marco-Urrea, E., Pérez-Trujillo, M., Vicent, T., Caminal, G., 2009. Ability of white-rot fungi to remove selected
506 pharmaceuticals and identification of degradation products of ibuprofen by *Trametes versicolor*. *Chemosphere.*
507 74, 765–772.
508
509 Mashkour, M., Rahimnejad, M., Mashkour, M., 2016. Bacterial cellulose-polyaniline nano-biocomposite: A
510 porous media hydrogel bioanode enhancing the performance of microbial fuel cell. *Journal of Power Sources.* 325,
511 322-328.
512
513 Mbokou, F.S., Kenfack Tonle, I., Pontié, M., 2017. Development of a novel hybrid biofuel cell type APAP/O₂
514 based on a fungal bioanode with a *Scedosporium dehoogii* biofilm. *J. Applied Electrochemistry.* 47, 273–280.
515 doi.org/10.1007/s10800-016-1030-5
516
517 Mbokou, F.S., Pontié, M., Razafimandimby, B., Bouchara, J.-P., Njanja, E., Tonle Kenfack, I., 2016a. Evaluation
518 of the degradation of acetaminophen by the filamentous fungus *Scedosporium dehoogii* using carbon-based
519 modified electrodes. *Anal. Bioanal. Chem.* 408, 5895-5903. DOI 10.1007/s00216-016-9704-8.
520
521 Mbokou, FS, Pontié M, Bouchara J-P, Tchieno MMF, Njanja E, Mogni A, Pontalier YP, Tonle KI 2016b.
522 Electroanalytical Performance of a Carbon Paste Electrode Modified by Coffee Husks for the Quantification of
523 Acetaminophen in Quality Control of Commercialized Pharmaceutical Tablets. *Int J Electrochem* Volume 2016,
524 Article ID 1953278, <http://dx.doi.org/10.1155/2016/1953278>
525
526

527 Morales, L.T., Gonzalez-Garcia, L.N., Orozco, M.C., Restrepo, S., Vives, M.J., 2017. The genomic study of an
528 environmental isolate of *Scedosporium apiospermum* shows its metabolic potential to degrade hydrocarbons.
529 *Stand. Genomic Sci.* 12, 71.
530

531 Morath, U. S, Hung R., Bennett W. J. 2012. Fungal volatile organic compounds: A review with emphasis on their
532 biotechnological potential. *Fungal Biology Reviews.* 26, 73-83.
533

534 Rahimnejad M., Adhami, A. Darvari, S. Zirepour, A., Oh, S.E. 2015. Microbial fuel cell as new technology for
535 bioelectricity generation: A review. *Alexandria Engineering Journal.* 54, 745-756.
536

537 Ghasemi, M., Wan Daud, W.R., Ismail, M., Rahimnejad M., Fauzi A., Leong, X., Miskan, M., Ben Liew, K.. 2013.
538 Effect of pre-treatment and biofouling of proton exchange membrane on microbial fuel cell performance.
539 *International Journal of Hydrogen Energy.* 38, 5480-5484.
540

541 Rahimnejad, M., Ghasemi, M., Najafpour D.G., Ismail, M., Mohammad, W.A., Ghoreyshi, A.A. Sedky H.A..
542 2016. Synthesis, characterization and application studies of self-made Fe₃O₄/PES nanocomposite membranes in
543 microbial fuel cell. *Electrochimica Acta.* 85, 700-706.
544

545 Oriez.V., Peydecastaing.J., Pontalier.P.I. 2019. Separation of sugarcane bagasse mild alkaline extract
546 components by ultrafiltration-membrane screening and effect of filtration parameters. *Process Biochemistry.* 78,
547 91-99. Doi: 10.1016/j.procbio.2019.01.006.
548

549 Pham, T., Giraud, S., Schuliar, G., Rougeron, A., Bouchara, J.-P., 2015. Scedo-Select III: a new semi-selective
550 culture medium for detection of the *Scedosporium apiospermum* species complex. *Med. Mycol.* 53, 512–519.
551

552 Potter: M.C, 1911 Electrical effects accompanying the decomposition of organic compounds, *Proc. R*
553 *Soc London*, B 84, 260-276
554

555 Prasad, D., Arun, S., Murugesan, M., Padmanaban, S., Satyanarayanan, R.S., Berchmans, S., Yegnaraman, V.,
556 2007. Direct electron transfer with yeast cells and construction of a mediatorless microbial fuel cell. *Biosens.*
557 *Bioelectron.* 22, 2604–2610. DOI:10.1016/j.bios.2006.10.028
558

559 Pollegioni, L., Tonin, F., Rosini, E., 2015. Lignin-degrading enzymes. *FEBS J.* 282, 1190–213.
560

561 Pontie, M., Mbokou, S., Bouchara, J.-P., Razafimandimby, B.J., Pontalier, P.Y., 2017. Paracetamol sensitive
562 cellulose-based electrochemical sensors. *J. Renewable materials.* 6, 242-250. doi.org/10.7569/JRM.2017.634169
563

564 Rodarte-Morales, A.I., Feijoo, G., Moreira, M.T., Lema, J.M., 2012. Biotransformation of three pharmaceutical
565 active compounds by the fungus *Phanerochaete chrysosporium* in a fed batch stirred reactor under air and oxygen
566 supply. *Biodegradation.* 23, 145–156.
567

568 Raghavulu, S. V., Goud, R. K., Sarma, P. N., & Mohan, S. V. 2011. *Saccharomyces cerevisiae* as anodic biocatalyst
569 for power generation in biofuel cell: influence of redox condition and substrate load. *Bioresource technology*,
570 102(3), 2751-2757.

571 Sekrecka-Belniak, A., Toczyłowska-Maminska, R., 2018. Fungi-Based Microbial fuel cells. *Energies*. 11,
572 2827-2845. doi:10.3390/en11102827.

573

574 Slate, A.J., Whitehead, K.A., Brownson, D.A.C., Banks, C.E.,2019. Microbial fuel cells: An overview of current
575 technology. *Renewable and Sustainable Energy Reviews*. 101, 60–81 and references therein.
576 doi.org/10.1016/j.rser.2018.09.044.

577

578 Zhang, L., Hu, J., Zhu, R., Zhou, Q., Chen, J., 2013. Degradation of paracetamol by pure bacterial cultures and
579 their microbial consortium. *Appl. Microbiol. Biotechnol.*97, 3687–3698. doi: 10.1007/s00253-012-4170-5.

580

581